Cent. Eur. J. Phys. • 8(2) • 2010 • 228-234
DOI: 10.2478/s11534-009-0151-4

VERSITA

Central European Journal of **Physics**

Spatial light modulator as a reconfigurable intracavity dispersive element for tunable lasers

Research Article

Lin Dong[12], Sergei Popov[1]*, Sergey Sergeyev[3], Ari T. Friberg[145]

1 *Royal Institute of Technology (KTH), Department of Microelectronics and applied Physics, SE-164 40 Kista, Sweden*

2 *Joint Research Center of Photonics (KTH/Zheijang University), Department of Microelectronics and applied Physics, SE-164 40 Kista, Sweden*

3 *Waterford Institute of Technology, Optics Research Group, Cork Road, Waterford, Ireland*

4 *Helsinki University of Technology, Department of Engineering Physics, FI-02015 TKK, Finland*

5 *University of Joensuu, Department of Physics and Mathematics, FI-80101 Joensuu, Finland*

Received 12 October 2008; accepted 17 September 2009

Abstract: An improved approach for narrow-band wavelength selection in tunable lasers is described. To provide the tunability, a reconfigurable diffractive optical element (DOE) based on a programmable spatial light modulator (PSLM) is applied. With a proper choice of the phase transfer function of the PSLM, the device can be used as a dispersive intra-cavity component for precise tuning within the lasing spectral band of a solid-state dye laser. The suggested design allows avoiding the mechanical movement of any cavity components. The tunability performance and simulation are demonstrated using the Fourier optics method.

PACS (2008): 42.40.Lx, 42.55.Mv, 42.79.Hp, 42.79.-e, 42.79.Dj

Keywords: spatial light modulator • diffractive optical element • tunable dye laser

1. Introduction

Tunable lasers, first of all, those incorporating organic dyes as a broadband gain material, require dispersive components to provide an accurate adjustment of the output lasing wavelength. With careful laser design, especially using solid-state dye materials as the gain media, it is possible to achieve extremely narrow-band output radiation [1–3]. Most of the methods to obtain fine tuning of the wavelength exploit bulk optical components, such as mirrors, diffractive grating and prisms, in which the tunability is realized with the movement (rotation) of the proper components. Since the 1960s, when first results of the tunable narrow-band emission from dye lasers were reported, dispersive elements typically used rotating mirrors and/or gratings [4, 5]. However, the best achieved lasing linewidth was not less than 0.4 Å in the early stages until the end of the 1970s when the combination of a holographic grating and Fabry-Perot etalon were used to suppress the radiation spectrum down to 0.01 Å [6, 7]. In 1978,

*E-mail: sergeip@kth.se

M. G. Littman *et al.* reported their improved, yet simplified, design with a spectral halfwidth of 1.25 GHz that corresponded to about 0.015 Å [8].

In this report, we describe an improved tuning system suitable for the wavelength adjustment in dye lasers. Using a programmable spatial light modulator (PSLM), a tuning resolution better than 1 nm within the wavelength range of 570 – 590 nm can be routinely achieved. The resolution can be further improved down to the order of 0.01 nm by using an advanced phase function control of the PSLM. In previous demonstrations, application of the binary PSLM for intra-cavity tuning provided the tunability of 1 nm at best [9]. Thus, our design using the 256-level phase retardation function in the considered PSLM offers a significant improvement in the tunability.

2. Design and main principle of the functionality

The tuning scheme considered in this paper is based on a well-known design [8]. The main advantage of our method is that a rotating back mirror providing wavelength selectivity in the classical solution, is now fixed, and a programmable, 8-bit addressable spatial light modulator is inserted between the back mirror and holographic grating (Fig. 1). Thus, the PSLM which operates as a dynamic diffractive optical element (DOE) with a properly adjusted phase function, is capable of creating a "synthesized" blazed grating to deflect different wavelength components separated by the holographic grating. This modification replaces the mechanical rotation of the cavity back mirror with a steering of the optical wavefront by electronically controlled PSLM to keep at least the same accuracy and speed of the tuning. To estimate the scheme feasibility, we consider a practical example of a simple solid-state dye laser containing a polymeric gain material of the wedge form with embedded Rhodamine 6G dye [10]. Such a laser with two flat cavity mirrors produced radiation with the central wavelength around 558 nm and with a full width of half maximum (FWHM) of 3 nm.

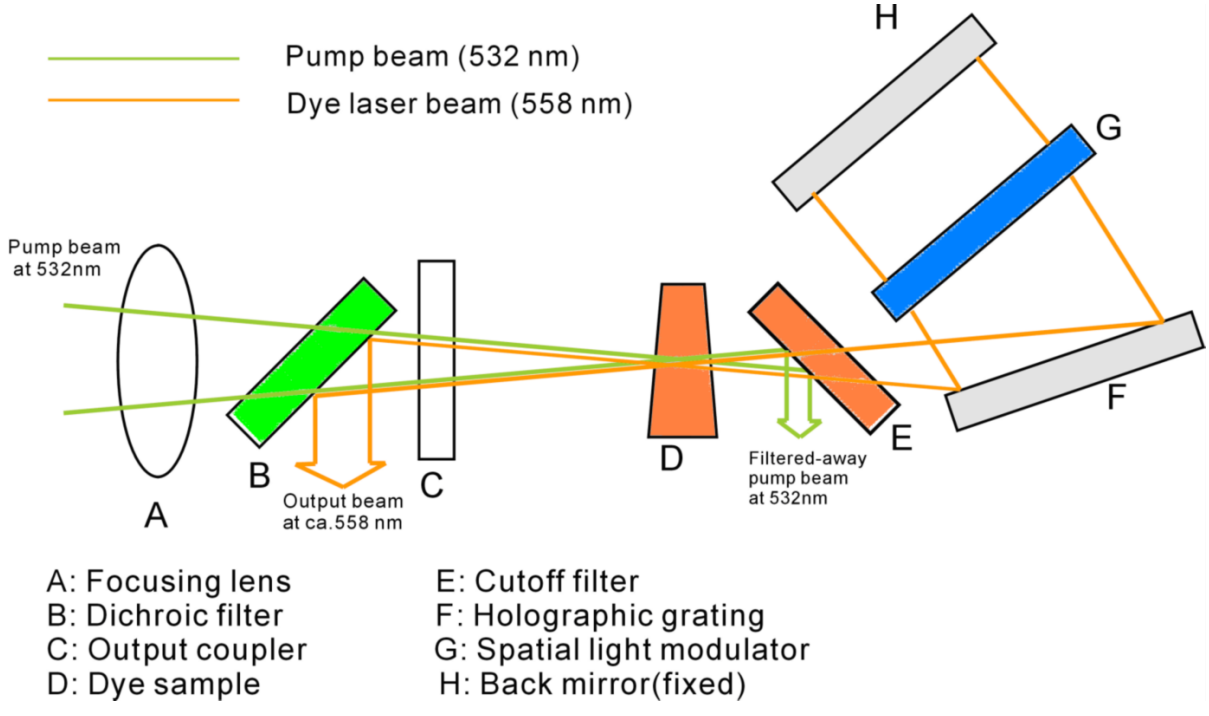

Figure 1. Schematic layout of a tunable solid-state dye laser with an intracavity dispersive component using the PSLM.

Starting with the design given in [8], we define the main parameters of the tunable scheme. A 50-mm wide holographic grating with a groove density of 1800 l/mm sep-

arates the spatially spectral components of the incident laser beam into different directions in the first diffraction order according to the grating equation

$$\sin\alpha + \sin\beta_m = -\frac{m\lambda}{d}, \tag{1}$$

and the dispersion equation

$$\frac{d\beta_m}{d\lambda} = \frac{-m}{d\cos\beta_m}, \tag{2}$$

where α and β_m are the angles of incidence and diffraction respectively, m denotes the (integer) number of the diffraction order, d is the groove spacing, and λ is the wavelength of the incident light. Using the numbers applied in our example, where m is -1, d is 1/1800 mm, λ is 558 nm and α is 89.2°, the angle of diffraction β_m produces the value of 0.257° (shown schematically in Fig. 2).

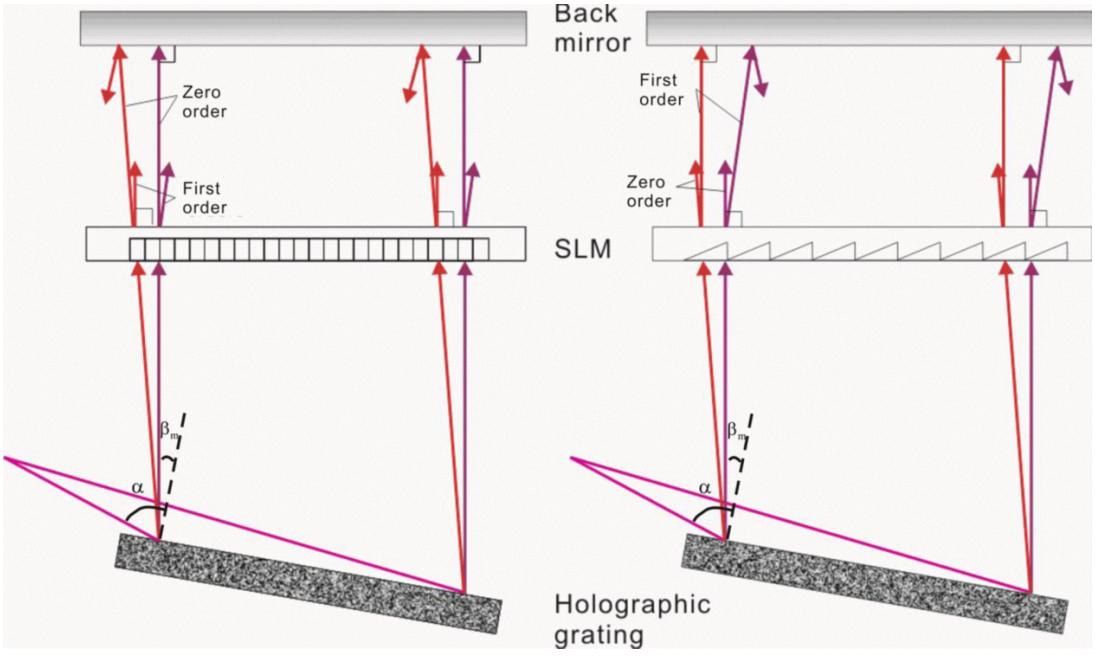

Figure 2. Control of spectral components in selected diffractive orders with the use of different patterns of the phase retardation function in the PSLM.

Setting these values into Eq. (2) and defining the difference between the two wavelength components $d\lambda$ of 1 nm, a spatial separating angle of 1.8 mrad between these two wavelength components should be obtained. The spectral width of each component is defined by the resolving power of the holographic grating according to following equation [8]

$$\frac{\Delta\lambda}{\lambda} = \frac{\lambda}{\pi l\sin\theta}, \tag{3}$$

where $\Delta\lambda$ is the half width of the spectral band of the light at wavelength λ, l is the width of the illuminated part of the grating, and θ is the angle of incidence. For the considered example, the bandwidth of each component is approximately 0.04 Å that is smaller than the required tuning range of 1 nm. Thus, the 1.8 mrad separation between neighbouring diffractive orders can guarantee no overlapping between different spectral components.

To realize the fine tunability between selected narrowband spectral components [8], the PSLM synthesizes an appropriate blazed grating to provide cavity resonance conditions, *i.e.*, ensuring normal incidence and reflection of the desired wavelengths from the back mirror. The PSLM used to manipulate the wave components separated by the holographic grating is LC-2002 from Holoeye Photonics Corporation [11]. This PSLM implements the functional-

ity of a programmable DOE with a size of 600×800 pixels with a 256-level phase modulation of each pixel, corresponding to the 256-step phase change between 0 and 2π. With a pixel size of 32×32 μm and fill-factor of 85%, such a PSLM can be considered a dynamic multiple-level holographic kinoform [12–14].

3. Modeling and experimental results

We analyze the functionality and perform an experimental test of the tuning scheme using the modulator LC-2002 and He-Ne laser with a wavelength of 633 nm. First, the typical dye laser radiation (e.g., using Rh6G dye) falls in the range between 530 and 633 nm, where the PSLM is designed to operate in pure phase modulation mode. This feature is favorable to avoiding the amplitude modulation of the PSLM and minimizing the intracavity optical losses. Thus, a very narrowband radiation from the He-Ne laser (about several MHz) is a perfect tool to test the spectral resolution of the tunable dispersion element employing the PSLM. The resolving power of the tuning system is mainly defined by the size of the holographic grating, which, in turn, is limited by the aperture of the PSLM (Fig. 2).

The main functioning part of the PSLM is a programmable DOE consisting of 600×800 pixels. Each pixel is a two-part structure, a 29.5 μm active area, which is responsible for letting the light through and implementing the phase modulation, and a 2.5 μm "dead" area which lies between two adjacent active parts. The "dead" areas are totally opaque to the incoming light, resulting in a periodic structure of the DOE. The basic period length G_s is the length of one 32 μm pixel. In our model, only one dimension of the DOE is considered. Following the structure periodicity, a perpendicularly incident beam is diffracted and split into plane waves with different directions. The angle between the two adjacent directions θ is related with G_s *via* the following ratio (valid for small angle approximation)

$$\theta = \frac{\lambda}{G_s}, \tag{4}$$

where λ is the wavelength of the incident light, 633 nm in this case. This results in θ being equal to 19.8 mrad for the PSLM parameters. To verify this, a lens of 28 cm focal length was put behind the PSLM to measure the sport deflections at the Fourier plane. Light spots at distances ca. 5.5 mm were found on the screen, which is close to the theoretical value $L = \theta \cdot f = 5.539$ mm.

To apply the Fast Fourier Transform (FFT) in the numerical modeling, a unit element in the space domain is chosen

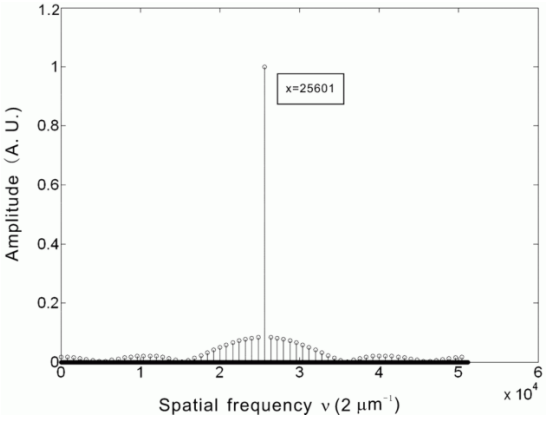

Figure 3. Spatial spectral distribution of the diffracted components with no pattern applied to the PSLM. X-coordinate (inside a box) denotes the position of highest diffractive order in units of discrete elements of FFT (corresponding to spatial frequencies).

with a size of $\rho = 0.5$ μm, which results in the unit value ν of 2 μm^{-1} in the spatial frequency domain. This allows the representation of both active and "dead" parts of one pixel as a multiplication of integer units. The Fourier spectrum after the PSLM is shown in Fig. 3. Thus, an optical beam after passing the PSLM is split into discrete directions with fixed separations corresponding to the peaks in the spectrum. This direction separation ϕ can be calculated as

$$\phi = \frac{m\upsilon\lambda}{51200}, \tag{5}$$

where $m = 800$ is the number of elements between adjacent peaks in Fig. 3 and 51,200 is the scaling factor to eliminate the influence from zero padding in the numerical calculation of the Fourier transform. With the PSLM data given above, the experimentally measured angle separation leads to $\phi = 9.8$ mrad that corresponds to the theoretical estimation. Meanwhile, the light energy is mainly concentrated in the direction of the zeroth diffraction order, *i.e.* the central peak, which coincides with the direction of the incident plane wave.

To redirect a separate wavelength component (in our case, a narrowband 633 nm radiation) into a certain diffractive order with high efficiency, we create a blazed grating pattern with period length $D = 10$ pixels in the PSLM. A particular number of 10 pixels for one "tooth" is chosen to match small deflection angles for different components. These wavelength components are separated in space by the holographic grating and get further diffracted by the PSLM each into different orders. When no grating pattern is applied onto the PSLM, the most energy is delivered to the zeroth orders (Fig. 2a). Alternatively, if the blazed

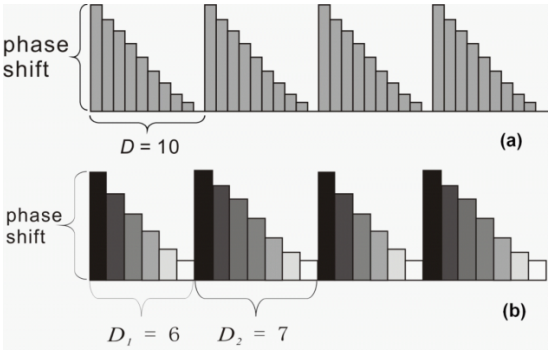

Figure 4. Examples of phase profiles inside grating unit cells. The phase shift is varied between 0 and 2π in each programmed pixel. (a) - grating pattern of equal cells with 10 pixels in each. (b) - improved pattern of the blazed diffractive grating using "6+7" interleaving scheme for the cell periods.

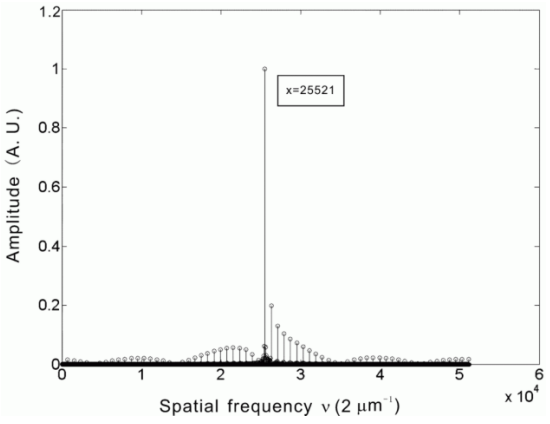

Figure 5. Spatial spectral distribution of the diffracted components with the "teeth" pattern (shown in Fig. 4a) applied to the PSLM. X-coordinate (inside a box) denotes the position of highest diffractive order in units of discrete elements of FFT (corresponding to spatial frequencies).

grating pattern is applied, the most energy is shifted to the first order (Fig. 2b). If this is the case, the wavelength component that is normal to the fixed back mirror in Fig. 2a would violate the cavity resonance condition and give it to another wavelength component whose first order is normal to the back mirror. The maximum phase shift of the PSLM pixel is set to 1.91π, which corresponds to a gray level value of 255 in the phase encoding scheme. Indeed, this is the maximum phase shift achievable for the 588 nm radiation (corresponding to the dye laser), since the nominal $2\ \pi$ -shift wavelength of the PSLM is designed for the 532 nm radiation. The gray level interval between 0 and 255 (0 to 1.91 π in terms of phase shift) is correspondingly divided into 10 steps and assigned onto 10 pixels in one period (Fig. 4a). It is worth noticing that such a virtual blazed grating is not expected to operate exactly as a real blazed grating with smooth teeth in terms of diffraction efficiency due to the discrete variation of the phase shift in each period.

The simulation result for the phase blazed grating with 10-pixel "teeth" is shown in Fig. 5. The main peak is shifted 80 elements away from the central point, indicating that the zeroth order is suppressed and this portion of energy (more than 80% of the total amount) is redirected to the first order. According to Eq. (5), deflection angle θ is 1.74 mrad, for $m = 80$, $\nu = 2\ \mu m^{-1}$ and $\lambda = 558$ m. This value is very close to the angle difference $\Delta\beta_{-1} = 1.8$ mrad for 1 nm tuning as discussed before. It is worth mentioning that this angle shift $\theta = 1.74$ mrad is valid for all the wavelength components which are separated by the holographic grating. In other words, the wavelength-dependent dispersion is small enough compared to θ, to be safely omitted. For the grating period of $D = 10$ pixels, the dispersion for the 1 nm wavelength difference results only in 0.0029 mrad according to the grating Eq. (3). For small incidence angles, the separation θ between two adjacent diffraction orders of the same wavelength should correspond to a spatial deflection of different wavelengths of the same diffraction order. According to Eq. (2) they should be equal to the wavelength difference between the two components coming from the holographic grating as $\Delta\lambda = 0.97$ nm. Thus, by applying the pattern with $D = 10$ pixels and $\varphi_m = 1.91\pi$ onto the PSLM, the output wavelength can be tuned by a range of 0.97 nm, which is the required accuracy for a solid dye laser system. The wavelength tuning is achieved by first aligning one of the wavelength components, denoted as λ_1, perpendicular to the back mirror, and then changing the pattern on the PSLM, *i.e.* the period D, to divert the wavelength components. Since all the components undergo a same angle shift θ, λ_1 loses the condition to be perpendicular to the back mirror and remises it to another wavelength component λ_2 which is exactly next to λ_1 with the angle θ all the time. This spectral component λ_2 becomes a new output wavelength (Fig. 2). With the same phase shift in PSLM pixels φ_m, but different D, other tuning range can also be achieved. The shapes of the spatial spectra remain similar to that shown in Fig. 5. The difference is the shift of n elements of the dominant peak away from the center and the distance between main peaks. The equivalent wavelength difference translated from n for $D = 1$-20 is shown in Fig. 6. From this graph, one can see that the tuning resolution improves when period D is increased.

Another noticeable feature can be observed from the diagram in Fig. 6. The tuning resolution is limited due to discrete gaps between adjacent points, which are reasons of

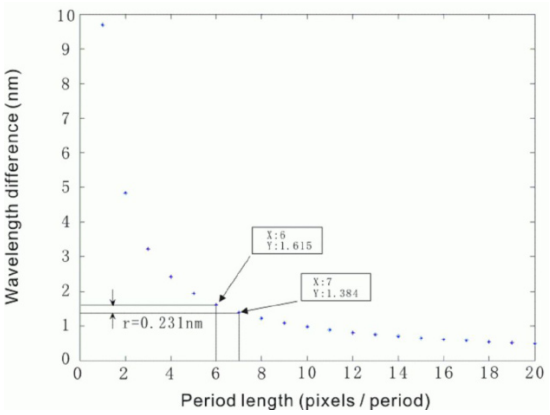

Figure 6. Dependence of the spectral resolution on the number of pixels in one period of the grating. X-value presents the number of modulator pixels in one period cell, Y is the corresponding wavelength resolution.

'quasi-real' blazed grating with discretized periods D. In order to improve the performance of the tuning approach, we introduce a non-equal interleaving scheme for periods D. Two adjacent blocks of pixels with D_1 and D_2 elements form the 2-period interleaving case with a new period $D = D_1 + D_2$ which is the basic structure of the pattern. For example, if $D_1 = 6$ and $D_2 = 7$ (Fig. 4b), then the tuning step is 1.49 nm, which falls between the tuning steps with $D = 6$ and $D = 7$ separately, *i.e.* between 1.61 nm and 1.38 nm, respectively. Thus, the distance of the main diffraction peak from the center point lies also between the two distances provided by D_1 or D_2 separately. Results for the 2-period interleaving tuning are shown in Fig. 7a. Increasing the number of blocks in the interleaving scheme allows further improving the tuning accuracy. The case with 3-component blocks, following the rule "6+6+7" and "6+7+7" elements is demonstrated in Fig. 7b. This feature makes it more flexible to define the tuning range and the corresponding resolution (of the order of 0.01 nm for 3-period interleaving).

Finer tunability with higher spectral resolution can be achieved with the use of more sophisticated patterns for "quasi-blazed" grating with larger amount of unit blocks in one "period". However, special attention should be paid to the diffraction efficiency since such patterns differ from classical blazed grating profile, and the highest possible efficiency in the first diffractive order is not guaranteed anymore.

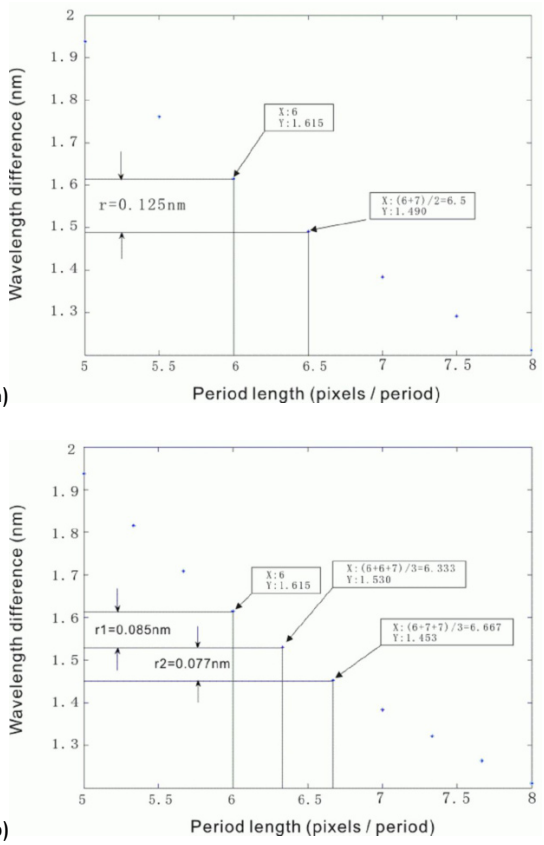

Figure 7. Increased spectral resolution obtained with an interleaved structure of the grating periods: application of (a) double interleaving pattern with 6+7 pixels, (b) double interleaving pattern of 6+6+7 and 6+7+7 pixels for one period. X-value presents the number of modulator pixels in one period cell, Y is the corresponding wavelength resolution.

4. Improved diffractive efficiency

The diffractive efficiency ε of the "quasi-blazed" grating can be easily calculated as the ratio of the energy of the main peak to the total energy. It is reasonable to assume that ε increases with D, since the teeth of the grating with a large period length get smoother and behave closer to that in a real blazed grating. This is justified by the calculation, which shows that for $D = 8$, 10, 16, diffractive efficiency ε is 83.65%, 87.09% and 90.48%, respectively. For the limiting case with $D = 800$, *i.e.*, the whole grating contains only one period, ε can reach 91.56%. Keeping in mind the previous analysis on the tuning resolution, one can naturally prefer a larger period length for the grating design. However, this is not the case if we consider other performance factors like the sweeping range of tuning. The grating with teeth of a large period is limited in the tilt angle, provided that the phase shift of the end

pixel can only vary in the range between 0 and 2π. This feature restricts the sweeping range that can be covered by the tuning. There exist different methods to circumvent this limitation, for example, choosing a smaller D and using the multi-period interleaving method to compensate for the resolution degradation, or application of the PSLM with smaller pixel size and larger number of pixels. In the latter solution, period length D can be kept relatively large to increase the tuning resolution together with the diffractive efficiency, and the sweeping range simultaneously.

The smallest pixel size of PSLM available today is around 8 μm. Compared with the PSLM in this report, the tuning resolution can be enhanced by a factor of 4. It is equivalent to inserting three extra points into every two adjacent points in Fig. 6, assuming that only the single period case is considered. Furthermore, the small pixel size helps to increase the number of discrete steps in each grating period, resulting in smoother grating teeth which are closer to those of a real diffractive grating. The diffractive efficiency is improved in this way.

5. Conclusion

An improved tuning scheme for dye lasers is considered in this report. The key dispersion element in the tuning system is an electronically controlled 8-bit addressing spatial light modulator which can act as a virtual blazed grating to manipulate the direction of the light waves passing by. With simple tests and numerical simulation, we demonstrated how a tuning resolution can be achieved up to 1 nm routinely, with a finer tuning of 0.01 nm using more advanced operations. The tuning system takes the merit of high speed and accuracy compared with traditional mechanical tuning systems and meanwhile shows no degradation in bandwidth compression. Although the PSLM has a limited number of only 800 pixels in the working area, a newly suggested interleaving scheme of the phase profile allows a significant increase in the tuning accuracy. A PSLM with smaller size and larger number of pixels can even further increase the tunability.

Acknowledgements

This work was financially supported by the Swedish Foundation for Strategic Research (SSF), the Academy of Finland (SA), and by the Enterprise Ireland Commercialisation Fund.

References

[1] F. J. Duarte, Appl. Optics 33, 3857 (1994)
[2] F. J. Duarte, Opt. Commun. 117, 480 (1995)
[3] F. J. Duarte, R. O. James, Opt. Lett. 28, 2088 (2003)
[4] B. H. Soffer, B. B. Mcfarland, Appl. Phys. Lett. 10, 266 (1967)
[5] H. Walther, J. L. Hall, Appl. Phys. Lett. 17, 242 (1970)
[6] F. P. Schäfer, H. Müller, Opt. Commun. 2, 407 (1971)
[7] M. Hercher, H. A. Pike, Opt. Commun. 3, 65 (1971)
[8] M. G. Littman, H. J. Metcalf, Appl. Optics 17, 2224 (1978)
[9] M. C. Parker, R. J. Mears, IEEE Photonic. Tech. L. 8, 1007 (1996)
[10] S. Popov, Appl. Optics 37, 6449 (1998)
[11] V. Arrizón, Opt. Lett. 28, 1359 (2003)
[12] A. Kolodziejczyk, Z. Jaroszewicz, A. Kowalik, O. Quintero, Opt. Commun. 200, 35 (2001)
[13] Z. Jaroszewicz, A. T. Friberg, S. Popov, J. Mod. Optic. 47, 939 (2000)
[14] G. Minguez-Vega, A. Thaning, V. Climent, A. Friberg, Z. Jaroszewicz, Proceedings of SPIE 4829, 1070 (2003)